Proceedings of the 2002 U.S. DOE Hydrogen Program Review
NREL/CP-610-32405

THERMOCATALYTIC CO_2- FREE PRODUCTION OF HYDROGEN FROM HYDROCARBON FUELS

N. Muradov
Florida Solar Energy Center
1679 Clearlake Road, Cocoa, Florida 32922
tel. 321-638-1448, fax. 321-638-1010, *muradov@fsec.ucf.edu*

Abstract

The main objective of this project is the development of an economically viable thermocatalytic process for production of hydrogen and carbon from natural gas or other hydrocarbon fuels with minimal environmental impact. The three major technical goals are: (i) to accomplish efficient production of hydrogen and carbon via sustainable catalytic decomposition of methane or other hydrocarbons using inexpensive, durable catalysts, (ii) to obviate the concurrent production of CO/CO_2 byproducts and drastically reduce (preferably, eliminate) CO_2 emissions from the process, and (iii) to produce valuable carbon products in order to reduce the cost of hydrogen production

The approach is based on thermocatalytic decomposition of hydrocarbons over carbon-based catalysts in an air/water-free environment. The important feature of the process is that the reaction is catalyzed by carbon particulates produced in the process, so no external catalyst is required (except for the start-up operation). This results in the following advantages: (1) no CO/CO_2 byproducts are generated during hydrocarbon decomposition stage, (2) no expensive catalysts are used in the process, (3) no catalyst regeneration is required (in contrast to metal catalyst-based processes), (4) several valuable forms of carbon can be produced in the process depending on the process conditions (e.g., turbostratic carbon, pyrolytic graphite, spherical carbon particles, carbon filaments etc.), (5) CO_2 emissions could be drastically reduced (compared to conventional processes).

The following is a brief description of major findings:

- The means for improving the catalyst long-term stability and process sustainability were determined. It was found that the process sustainability could be improved using two approaches: (i) the in-situ generation of catalytically active carbon species produced by co-decomposition of methane and unsaturated and/or aromatic hydrocarbons, and (ii) reactivation of carbon catalysts via surface treatment with activating agents, e.g., steam and/or CO_2.
- The effect of moisture and sulfur compounds present in commercial hydrocarbon fuels on the process efficiency and the catalyst activity and stability was determined. It was demonstrated that the presence of small amounts of moisture and sulfur in the feedstock is not detrimental for the process efficiency. However these impurities may result in contamination of hydrogen by CO, CO_2 and H_2S which should be removed from the product gas using methanation and H_2S scrubbing steps, respectively.

- A bench-scale thermocatalytic reactor (TCR) for CO/CO_2-free production of hydrogen-rich gas was designed, fabricated and operated using methane or propane as feedstocks. TCR produced gases with H_2 concentration up to 80 v.%, balance- CH_4.
- TCR was tested in combination with PEM fuel cell. It was demonstrated that the TCR-produced hydrogen gas could be directly fed to PEM fuel cell with no need for gas conditioning (e.g., water gas shift, preferential oxidation) and gas separation stages required by conventional technologies (e.g., steam reforming, partial oxidation).
- Carbon products of the process were analyzed by a number of material characterization techniques, including XRD, SEM, AES, XPS, EDS, DR- FTIR. The market value of the carbon products were evaluated.
- Techno-economic analysis of hydrogen and carbon production by thermocatalytic decomposition of natural gas was conducted in cooperation with NREL. It was determined that hydrogen could be produced at a selling price of $7-21/GJ depending on the cost of natural gas and carbon selling price.

INTRODUCTION

Thermal (or thermocatalytic) decomposition (TCD) of NG occurs at elevated temperatures and results in the formation of hydrogen and elemental carbon:

$$CH_4 \rightarrow C + 2H_2 \qquad \Delta H^o = 75.6 \text{ kJ/mol } (CH_4) \qquad (1)$$

Due to the absence of oxidants (e.g., H_2O and/or O_2) no carbon oxides are formed in the reaction. Thus, the main advantages of this approach relate to the production of hydrogen in a single step, with no need for gas conditioning (e.g., water gas shift, preferential oxidation) and gas separation (e.g., CO_2 removal) stages required by conventional technologies (e.g., steam reforming, partial oxidation, autothermal reforming). Methane decomposition is a moderately endothermic reaction. The energy input requirements per mole of hydrogen for TCD is significantly less than that of steam methane reforming (SMR) (37.8 and 63.3 kJ/mol H_2, respectively). Figure 1 compares the net hydrogen yield for TCD and SMR processes (with and without CO_2 sequestration). It can be seen that although theoretical hydrogen yield for SMR is twice of that for TCD (H_2/CH_4=4 and 2 mole/mole, respectively), high reaction endothermicity and CO_2 sequestration (both consume significant amount of energy in methane equivalent), would considerably reduce the net yield of hydrogen produced by SMR process.

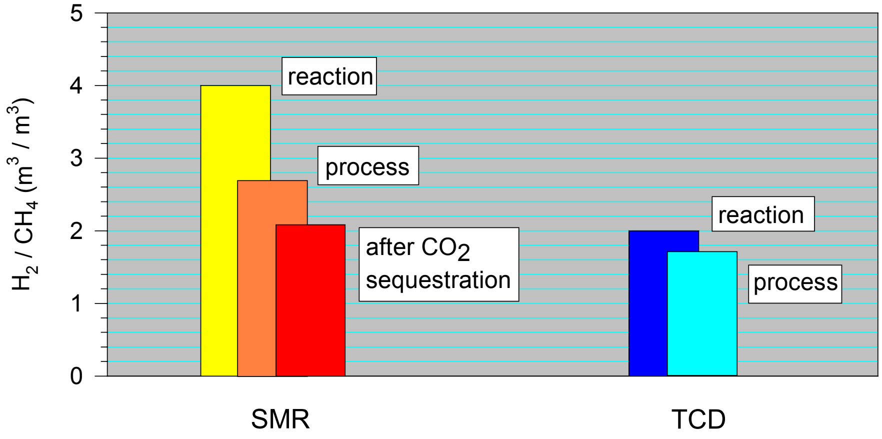

Figure 1. Comparative Assessment of Net Hydrogen Yields for SMR and TCD processes

According to Steinberg, the overall net energy efficiencies of TCD and SMR processes become close (58 and 60%, respectively) after accounting for 15% energy loss due to CO_2 sequestration [1]. Thus, both the overall energy efficiencies and hydrogen yields for TCD and SMR (after CO_2 sequestration) become fairly close. One should consider, however, that TCD process produces a valuable byproduct carbon, whereas, in SMR process 40% of the energy is lost irreversibly due to high reaction endothermicity and CO_2 sequestration stage. Carbon byproduct could potentially be sold, thus reducing hydrogen production cost.

Thermal decomposition of methane occurs at elevated temperatures (up to 1400°C), which lends itself to the use of catalysts in order to reduce the maximum temperature of the process and improve the process kinetics. Therefore the choice of an efficient and durable methane decomposition catalyst is vital for the development of TCD process. It is well known that the use of transition metal catalysts (e.g., Ni, Fe, Co, Pd) could significantly reduce the temperature of methane decomposition reaction [2-4]. However there is a catalyst deactivation problem associated with the carbon build-up on the catalyst surface. In the majority of cases carbon produced during hydrocarbon decomposition stage was combusted with air, providing heat for the endothermic reaction (e.g., [5]). This, however, results in contamination of hydrogen with carbon oxides and the production of CO_2 byproduct in quantities comparable with that of SMR.

The successful development of efficient and stable carbon-based catalysts for methane decomposition process can potentially solve both the catalyst deactivation and CO_2 emission problems. Carbon catalysts offer the following advantages over metal catalysts: (i) no catalyst regeneration is required, (ii) no sulfur poisoning, (iii) high fuel flexibility, (iv) production of a valuable byproduct carbon, and (v) significant reduction in CO_2 emissions. The detailed information on the catalytic properties of carbon catalysts for methane decomposition reaction has been published elsewhere (e.g., [6-8]).

EXPERIMENTAL

Reagents

Methane (99.99 v.%, Air Products and Chemicals, Inc.) and propane (99.0 v.%, Praxair) were used without further purification. Samples of activated carbons were obtained from Barneby Sutcliffe Corp., NORIT Americas and Kanzai Coke & Chemicals. Cabot Corp. provided different samples of carbon black. Graphites, glassy carbon and acetylene black were obtained from Alfa Aesar and used without further purification. All carbon samples were used in the form of fine powder (<100μm).

Apparatus

The experimental set-up for hydrocarbon fuel decomposition consists of 3 main subsystems: (1) a thermocatalytic reactor (with temperature-controlled electric heater and pre-heater), (2) a hydrocarbon metering and delivery sub-system, and (3) an analytical sub-system. All catalytic reactors were made out of a fused quartz or ceramic (alumina) in order to reduce the effect of the reactor material on the rate of hydrocarbon decomposition. The reactor temperature was maintained at a constant temperature via a type K thermocouple and Love Controls microprocessor. Hydrocarbon flow rates were metered by Gilmont flow meters. Proton Exchange Membrane (PEM) fuel cell was manufactured by the Energy Partners Inc. (West Palm Beach, FL). The description and operation of the experimental unit in more details is given in the Results and Discussion section.

Analysis

The analysis of the products of hydrocarbon decomposition was performed gas chromatographically: SRI- 8610A (a thermal conductivity detector, Ar carrier gas, a silica gel column, temperature programming from 25 to 180^{o}C), and Varian-3400, flame ionization detector, He-carrier gas, stationary phase- Hysep D_B. Aromatic (including, polynuclear) byproducts of hydrocarbon pyrolysis were analyzed spectrophotometrically (Shimadzu UV-2401PC). Characterization of carbon products was conducted at the Universal Oil Products (UOP), Materials Characterization Facility (MCF) and CREOL of the University of Central Florida, and AMIA Laboratories. The following materials characterization techniques were used for the structural and surface analysis of carbon samples: XRD, XPS, AES, SEM, EDS, DR-FTIR.

RESULTS AND DISCUSSION

Studies on the Improvement of Catalyst Stability and Process Sustainability

In-situ Generation of Catalytically Active Carbon Species
It was previously determined that major factors contributing to carbon catalyst deactivation were: blocking of active sites by catalytically inactive carbon particulates, and the reduction in catalytic surface area. It was found that the rate of catalyst deactivation depends on the nature of carbon catalyst and hydrocarbon and the operational parameters (e.g., temperature). Particularly, at higher temperatures (e.g., >850^{o}C) the pace of catalyst deactivation in methane decomposition reaction noticeably decreases compared to moderate temperatures (750-850^{o}C). Activated carbon (AC) catalysts demonstrated both the highest initial activity and, unfortunately, the highest rate of deactivation among all the carbon samples tested. In contrast, the initial rate of methane decomposition over amorphous carbons (e.g. carbon blacks, CB, and acetylene black), was somewhat lower than that of AC samples, but the rate of deactivation was also slower. CB-catalyzed methane decomposition reached a quasi-steady state rate (over 10-20 min) and remained practically stable for several hours, followed by the gradual decline in the reaction rate.

The above experimental results can be explained as follows. The catalytic activity of carbons in hydrocarbon decomposition is determined by the size of carbon crystallite and its structure, which in turn are governed by the temperature and the nature of hydrocarbon. Particularly, the size of the carbon crystallite produced during thermal decomposition of methane is an inverse function of the reaction temperature: higher is the temperature, smaller are the carbon crystallites. The total rate of the methane decomposition reaction is the sum of the rates of carbon nuclei formation and carbon crystallites growth. The rate of carbon nuclei formation is proportional to the substrate surface area: carbons with high surface area (e.g. ACs and some CBs) tend to have high initial catalytic activity. It was determined that the activation energy of the carbon nuclei formation during methane thermal decomposition (316.8 kJ/mole) is much higher than the activation energy of the carbon crystallites growth (227.1 kJ/mole) [9]. Thus, in general, the rate of carbon crystallites growth tends to be higher than the rate of carbon nuclei generation. With the rise in the temperature the mean size of carbon crystallites tends to decrease resulting in the increase in methane decomposition rate. This explains the experimental fact that at high temperatures (e.g., >850^{o}C) carbon catalysts tend to deactivate at slower rate compared to lower temperatures.

Rapid deactivation of AC catalysts can be explained by blocking of AC pores by growing carbon crystallites which hinder the internal diffusion of methane molecules. Pore diffusion controlled reaction could also be responsible for the insensitivity of methane decomposition rate to the origin and surface area of ACs. In contrast, the most of CB surface is relatively easily accessible to methane molecules during decomposition reaction. CBs differ in particle size, average aggregate mass, morphology, etc. (e.g. the oil furnace process produces CBs with particle diameters in the range of 10-250 nm, and surface area of 25-1500 m^2/g). CBs with high external surface area (e.g. BP-2000) result in relatively high steady state methane decomposition rate. The process could go on for several hours until most of the surface is covered with carbon crystallites produced from methane. It was estimated that it would take almost three hours to cover the surface of CB (BP-2000) with carbon species produced from methane (which is in acceptable agreement with the experiment). After 3-4 hours we observed gradual decrease in methane decomposition rate, due to rapid carbon crystallite growth and reduction in the catalytic surface area.

It was determined that carbons produced by thermal decomposition of different hydrocarbons exhibit dissimilar catalytic activities in methane decomposition reaction. In particular, the catalytic activity of carbons produced from different hydrocarbons can be arranged in the following order:

naphthalene > benzene > ethylene > propane > methane

The accelerating effect of ethylene and benzene on the methane decomposition rate is shown in Figure 2. In this series of experiments methane and methane-hydrocarbon mixtures were thermally decomposed over the surface of an inert support (SiO_2) at 850°C. It is clear that in the presence of ethylene and benzene methane decomposition rate increases two and seven fold, respectively.

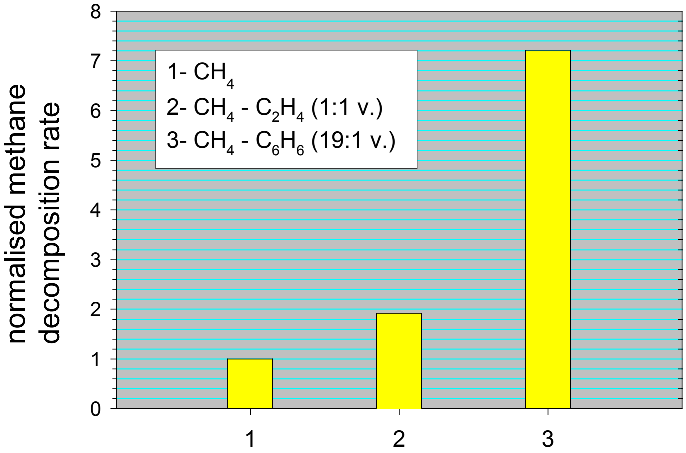

Figure 2. Effect of Ethylene and Benzene on Methane Decomposition Rate at 850°C

It was shown that the activity of carbon crystallites in methane decomposition reaction is a reverse function of their size: smaller crystallites are catalytically more active than larger ones. Thus, the rate of methane decomposition over relatively small crystallites (2-3 nm) produced from ethylene or benzene is higher compared to that of relatively large crystallites (approx. 100 nm) produced from methane.

The following theoretical considerations explain the effect of hydrocarbons (e.g., ethylene) on methane decomposition rate. The mean size of carbon crystallite (L_n) and the surface density (N_n) of crystallites in the n^{th} layer of carbon can be found from the following expressions [9]:

$$L_n = 2W\tau_n \tag{2}$$

$$N_n = P_{n-1}\tau_n U \tag{3}$$

where, W is the rate of crystallite growth, τ_n - time required for the formation of n^{th} layer, P- perimeter of the carbon crystallite, U- the rate of nuclei formation

Considering that

$$N=1/L_a^{2} \tag{4}$$

$$P=4L_aN/2 \tag{5}$$

$$P=2L_a \tag{6}$$

and

$$L_n = (L_{n-1}\frac{W}{U})^{1/3} \tag{7}$$

$$V=2d(UW)^{1/2} \tag{8}$$

$$L_a=\left(\frac{W}{U}\right)^{1/2} \tag{9}$$

(where L_a is a mean carbon crystallite size on the plane; V is rate of carbon growth in the direction normal to the plane; d is distance between graphitic layers)

the following expressions can be obtained for the growth of carbon crystallites from methane decomposition on the surface of carbon crystallites produced from ethylene:

$$\frac{L_n}{L_{CH_4}} = \left(\frac{L_{n-1}}{L_{CH_4}}\right)^{1/3} \tag{10}$$

$$L_n = L_{CH_4}\left(\frac{L_{C_2H_4}}{L_{CH_4}}\right)^{1/3^n} \tag{11}$$

Multiplying equation (8) by (9)

$$V_n L_n = V_{CH_4} L_{CH_4} = 2Wd \tag{12}$$

and comparing (11) and (12)

$$V_n = V_{CH_4} \left(\frac{L_{CH_4}}{L_{C_2H_4}} \right)^{1/3^n} \tag{13}$$

The equations (11) and (13) allow to determine the mean size and growth rate of carbon crystallites for *n*-th carbon layer. Evidently,

at $n \rightarrow \infty$ $V_n \rightarrow V_{CH4}$ and $L_n \rightarrow L_{CH4}$

These considerations explain the experimental fact that the rate of methane decomposition over small carbon crystallites obtained from ethylene is higher than a stationary rate; however, after reaching the steady state regime ($n \rightarrow \infty$) the kinetics of the process is governed by the rate of growth of carbon crystallites produced from methane.

The accelerating effect of olefins and aromatics on methane decomposition rate could advantageously be used to improve the process sustainability of hydrogen production from natural gas. This can be accomplished by recycling the gaseous stream containing methane-C_2+ mixture back to the reactor after hydrogen separation (see Figure 3).

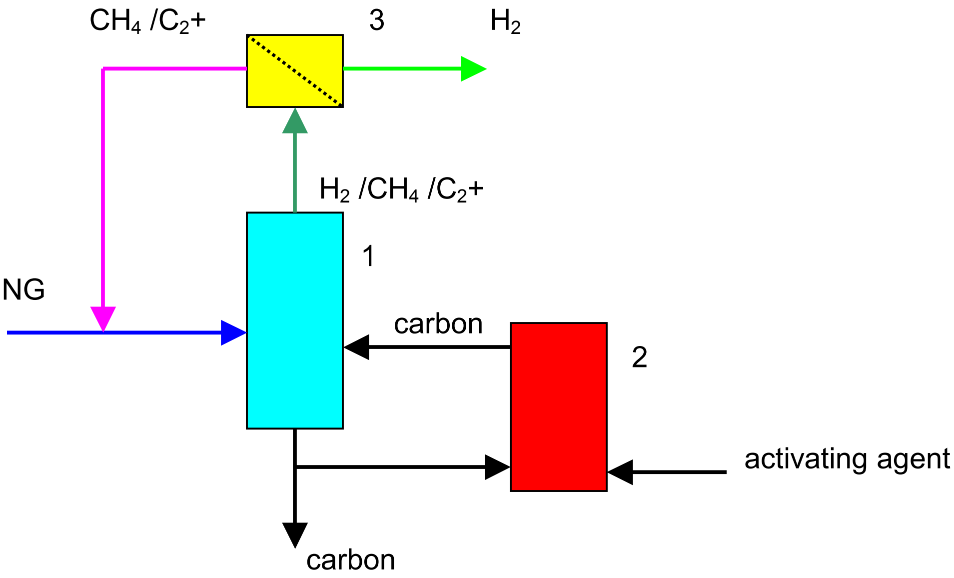

Figure 3. Simplified Block-diagram of TCD of NG 1- fluidized bed reactor, 2- fluidized bed heater, 3- gas separation unit

The experiments with the simulated NG feedstock (e.g., gaseous mixtures comprising 90 v.% CH_4 and 10 v.% C_3H_8) demonstrated that the effluent gas after the catalytic reactor contains noticeable amounts of ethylene, benzene, naphthalene vapors and other C_2+ compounds (up to 10 v.% and higher, depending on the operational conditions). After the separation of hydrogen, these heavy components of NG pyrolysis gas are recycled to the reactor where they are decomposed with the production of catalytically active carbon species resulting in the acceleration of methane decomposition reaction. We call this mode of increase in the catalytic activity of carbon catalysts the "in-situ" activation, since it takes place in the reactor during methane decomposition stage.

Reactivation of Carbon Catalysts Using Activating Agents

As discussed earlier, one of the main factors leading to deactivation of carbon catalysts relates to the drastic reduction in catalytic surface area during methane decomposition. In principle, the surface area of carbon particulates can be increased via their surface treatment with activating agents at elevated temperatures. High temperature steam, CO_2 or their mixtures are the most common activating agents in the production of activating carbons from a variety of carbonaceous materials.

In our work we attempted to apply this approach to increase the surface area and, consequently, catalytic activity of carbon particulates in methane decomposition reaction. In particular, we studied the effect of carbon catalyst activation on the rate of methane decomposition using several oxidizing agents: air, steam, CO_2 and steam-CO_2 mixtures. In this series of experiments the deactivated carbon samples (after exposure of a carbon catalyst to methane at 850°C for more than 6 h) were subjected to the treatment by equimolar amounts of steam, CO_2 and O_2 (air) at 950°C. The effect of carbon activation on methane decomposition rate is shown in Figure 4. It is evident that the treatment of carbon particles with steam and steam-CO_2 (1:1 by volume) mixtures resulted in significant increase in methane decomposition rate. Air exhibited a relatively low carbon activating efficiency.

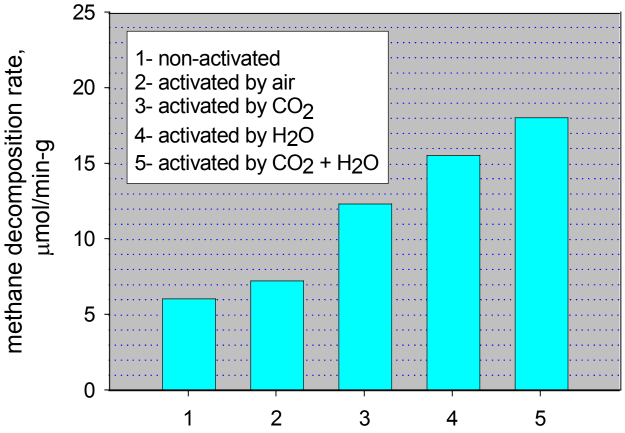

Figure 4. Effect of Carbon Catalyst Activation by Different Activating Agents on the Methane Decomposition Rate at 850°C. Activation Temperature 950°C

In principle, the activation of carbon particles with activating agents can be accomplished in the heater (see Figure 3) where temperature conditions (900-1000°C) are suitable for the activation process. Since the catalyst activation occurs outside the catalytic reactor we call this operation the "external" activation (to distinguish it from "in-situ" activation taking place within the reactor). Thus, both "in-situ" and "external" catalyst activation mechanisms can contribute to the improvement in the process sustainability. It is important to note that these two modes of catalyst activation act independently and potentially can complement each other.

Effect of Moisture and Sulfur on Methane Decomposition Rate

The objective of this task is to determine the effect of moisture, sulfur and other impurities present in commercial hydrocarbon fuels on the process efficiency. Potentially, these compounds can affect the catalyst activity and stability and contaminate hydrogen with reactive impurities, e.g., CO, H_2S, etc.

Effect of Moisture

Moisture is likely to be present in various quantities in the industrial grade (commercial) hydrocarbon fuels. We studied the effect of small amounts of water vapor on the rate of methane decomposition over the carbon catalyst (CB, BP2000). It was found that the introduction of small amounts (2.4 v.%) of water in the methane feedstock at the operational conditions of the thermocatalytic reactor (800-900°C) resulted in the formation of carbon oxides (CO and CO_2). The control experiments revealed that carbon oxides are produced via reaction of steam with carbon rather than with methane (thus, the contribution of methane steam reforming into the overall process is negligible). The important observation was that the presence of small amounts of water vapor in methane noticeably reduced the rate of catalyst deactivation. The positive effect of water vapor on methane decomposition rate can be attributed to the increase in catalytic surface area of carbon particulates via surface steam gasification (Fig. 5). From this point of view, the effect might be similar to that discussed in the previous section.

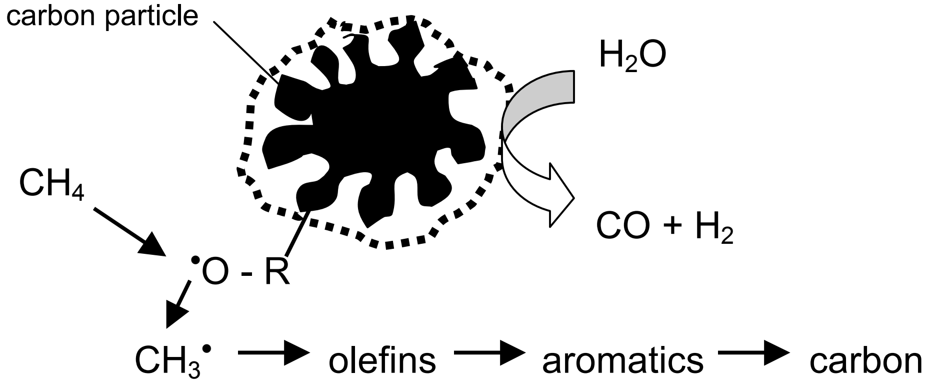

Figure 5. Reaction Scheme Explaining Effect of Water Vapor on Methane Decomposition Rate over Carbon Particles

However, other factors can also contribute to the accelerating effect of water vapor on methane decomposition reaction rate. For example, it is conceivable that active radicals can be generated on the carbon catalyst surface in the presence of such an oxidizing agent as water.

These radicals are capable of attacking methane molecules at elevated temperatures with the formation of methyl radicals which initiate the chain of consecutive reactions leading to production of carbon, as shown in Figure 5.

The presence of CO/CO_2 impurities in hydrogen gas in many cases might be undesirable (e.g., CO even in trace quantities deactivates PEM fuel cell). Fortunately, in small quantities, carbon oxides can be efficiently removed from hydrogen via methanation reactions:

$$CO + 3H_2 \rightarrow CH_4 + H_2O \qquad \Delta H^o = -251 \text{ kJ/mole} \qquad (14)$$

$$CO_2 + 4H_2 \rightarrow CH_4 + 2H_2O \qquad \Delta H^o = -253 \text{ kJ/mole} \qquad (15)$$

These reactions occur at relatively low temperatures (300-400°C) and require the presence of Ni- or Ru-based catalysts. The experiments indicated (see Figure 6) that carbon oxides could be practically removed from the hydrogen-methane stream with the aid of a methanator using an alumina-supported Ru-catalyst and operating at 350°C. It can be seen that CO concentration dropped from 2500 ppmv (before) to approx. 3 ppmv (after methanator).

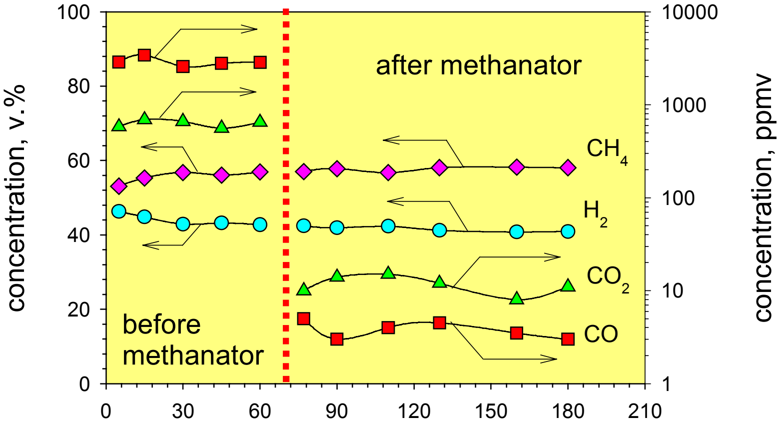

Figure 6. Removal of Carbon Oxides from H_2-CH_4 Stream via Methanation Reaction at 350°C in the Presence of Ru (0.5%)/Al_2O_3

Effect of Sulfur

It is well known that the presence of even small amounts of sulfur compounds in hydrocarbon feedstocks is detrimental for the activity of the majority of industrial catalysts (e.g., Ni-based catalysts). In most cases (e.g., steam methane reforming), an additional costly stage of feedstock desulfurization is included in the technological scheme in order to avoid rapid deactivation of metal catalysts.

We studied the effect of H_2S on the rate of methane decomposition over carbon catalysts. It was found that the presence of small amounts of H_2S in methane stream does not deactivate the carbon catalyst. The control experiments with Ar-H_2S mixtures demonstrated that H_2S is thermally decomposed over the surface of carbon catalyst (e.g., CB BP2000) at the temperature range of 850-900°C. Figure 7 demonstrates the effect of H_2S in the amount of 3 v.% on the rate of methane decomposition over CB(BP2000) catalyst at 870°C. It can be seen that during introduction of H_2S into methane stream the hydrogen concentration in the effluent gas increased by approx. 2-3 v.% which can be attributed to the contribution of hydrogen produced by thermal decomposition of H_2S.

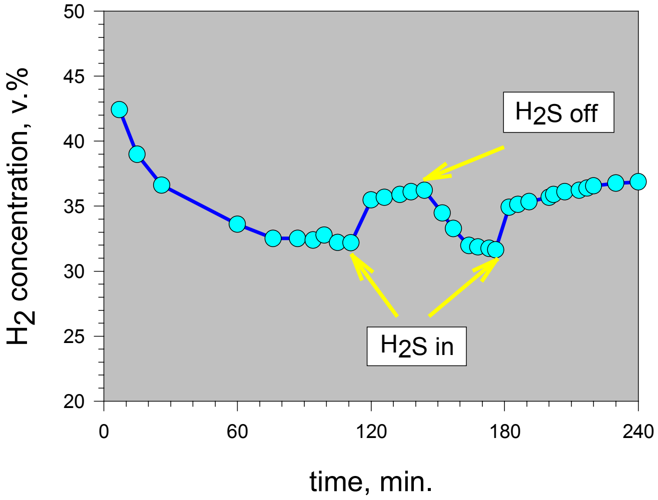

Figure 7. Effect of H_2S on Methane Decomposition over CB (BP2000). $[H_2S]$= 3 v.%, T= 870°C

It is also evident that in the presence of H_2S methane decomposition rate slightly increases which points to a possible accelerating effect of H_2S on methane decomposition reaction. An effect of H_2S on methane decomposition can tentatively be explained in terms of intermediate formation of relatively active $HS^\bullet$-radicals which attack methane molecules at elevated temperatures. The following reaction scheme explains the probable role of H_2S:

$$H_2S \rightarrow HS^\bullet + H^\bullet \qquad (16)$$

$$nHS^\bullet \rightarrow S_n + n/2H_2 \qquad (17)$$

$$CH_4 + HS^\bullet \rightarrow {}^\bullet CH_3 + H_2S \qquad (18)$$

Elemental sulfur (S_n) vapors exit the reactor and condense in a sulfur trap. Unconverted H_2S could be removed from the hydrogen stream by several of-the-shelf technologies, e.g., MEA scrubbing or ZnO polishing:

$$ZnO + H_2S \rightarrow ZnS + H_2O \qquad (19)$$

Fabrication and Testing of Thermocatalytic Reactor

A bench-scale thermocatalytic reactor (TCR) for CO/CO_2-free production of hydrogen-rich gases was designed, fabricated and tested at the Florida Solar Energy Center. The TCR employed a carbon-based catalyst; its design is proprietary (a U.S. Patent Application No. 60/203370 has been filed before U.S. PTO). Figure 8 depicts a simplified schematic diagram of the experimental set-up for testing TCR coupled with PEM fuel cell. The set-up consists of a TCR, a series of flow meters (rotameters) for measuring flow rates of a hydrocarbon feedstock (or fuel gas), an inert gas (Ar) and air, a series of valves, a PEM fuel cell, and a testing and analytical (GC) equipment. The photo of the experimental set-up assembled at FSEC is shown in Figure 9. The flow rate of hydrocarbon gas (methane or propane) varied in the range of 0.5-5 l/min. Ar was used to purge a reactor and PEM fuel cell before introducing a fuel gas. The temperature in the TCR was maintained at 800-900°C, at the atmospheric pressure.

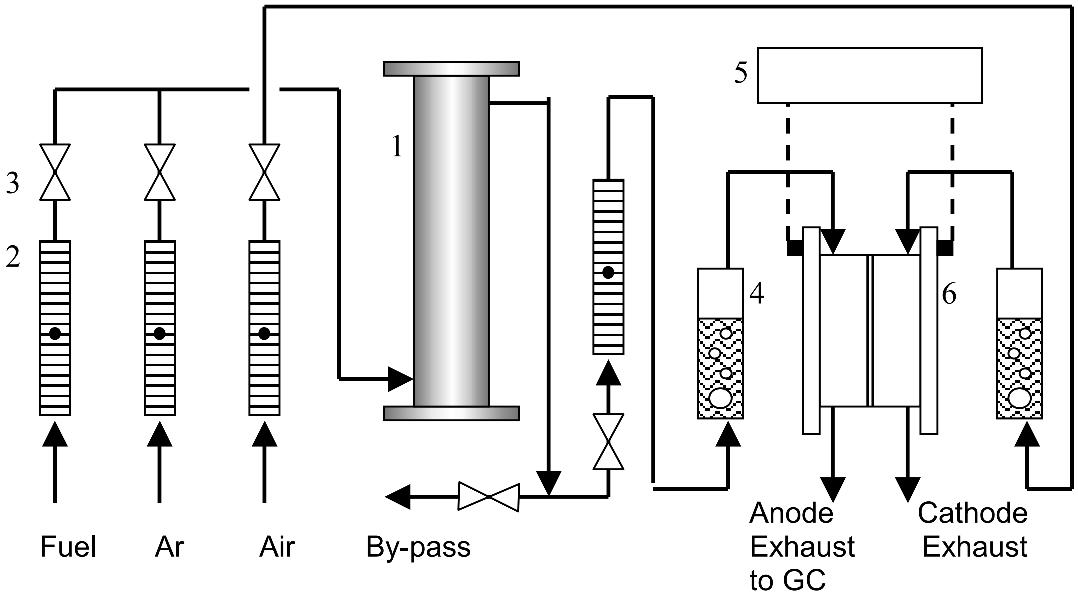

Figure 8. Schematic Diagram of the Experimental Set-up with TCR and PEM Fuel Cell TCR, 2- Flow meters, 3- Valves, 4- Humidifiers, 5- Electrical load with meters, 6- PEM fuel cell

A flow of hydrocarbon gas (e.g., methane or propane) enters TCR from the bottom section and is decomposed over the surface of a carbon-based catalyst producing hydrogen-rich gas which exits TCR via a ceramic filter. The concentration of hydrogen in the hydrogen-containing gas (HCG) depends on the feedstock, the reactor temperature and the residence time. Propane produces HCG with the concentration of hydrogen up to 70-80 v.%, the balance being methane and traces of C_2+ (depending on the flow rate). In case of methane, hydrogen content of the pyrolysis gas was somewhat lower (40-60 v.%, the balance-unconverted methane). No carbon oxides were detected in the pyrolysis gases. Since hydrogen gas was free of carbon monoxide (CO) and other reactive impurities, it was directly fed to a PEM fuel cell.

A single cell PEM fuel cell was used in this series of experiments. Since the power range of the PEM fuel cell was much lower compared to the output of TCR, only a small portion of the TCR effluent gas (in the range of 100-500 mL/min) was directed to an anode compartment of PEM fuel cell (via a bubble humidifier). A flow of air (0.5-2.5 L/min) was introduced into the cathode compartment of the fuel cell. PEM fuel cell and both humidifiers were maintained at 80°C. The exhaust gases from anode and cathode compartments of PEM fuel cell passed through condensers, where most of the moisture was condensed, and the flow rates of both exhaust gases were measured. The anode exhaust gas was directed to a GC analyzer where H_2 concentration was quantified. PEM fuel cell electrodes were connected to an electrical resistance load equipped with the meters for measuring cell potential and electrical current.

Figure 9. Experimental Set-up with TCR, PEM Fuel Cell, Fuel Tank and Testing Equipment

The cell potential *vs* current curves were plotted for the TCR-produced hydrogen-containing gases with the average hydrogen concentrations of 43, 60 and 79 v.% (balance- methane) (Figure 10 A). The plots "cell potential vs current" are typical of PEM fuel cell curves with activation, ohmic and concentration polarization regions. It can be seen that the dissimilarity in the behavior of different *i-v* plots showed up most vividly in the concentration polarization region.

We also monitored the concentrations of hydrogen in the fuel cell anode exhaust gas (Figure 10 B). It was demonstrated that the rate of hydrogen consumption in PEM fuel cell was a function of hydrogen concentration in the pyrolyzate gas and the fuel gas throughput. At low feed flowrates (e.g., 100-200 mL/min) almost all the hydrogen was consumed in the fuel cell, regardless of the original hydrogen concentration in the feed gas. At relatively high flowrates (e.g., 500 mL/min), however, a significant portion (almost half) of hydrogen exited the anode compartment of the fuel cell unconverted. The presence of methane in the feed gas in the whole range of its concentrations (20-60 v.%) did not adversely affect the performance of the fuel cell.

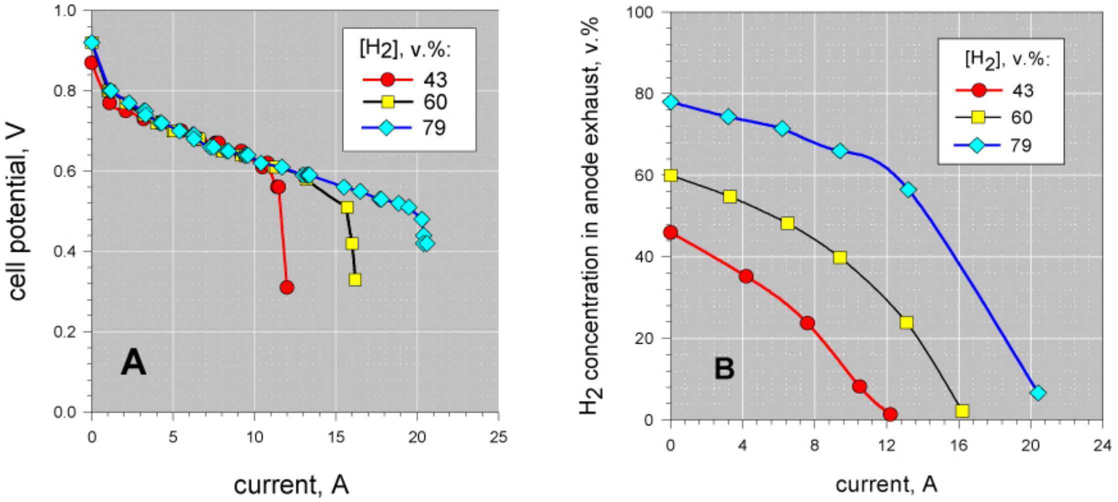

Figure 10 Testing of TCR Coupled with PEM Fuel Cell (Single Cell). Cell potential *vs* current curves for PEM fuel cell, (B) The effect of electrical load on H_2 concentration in the anode exhaust gas

Structural and Surface Characterization of Carbon Products

X-Ray Diffraction Studies of Carbon Samples

We conducted X-ray diffraction (XRD) studies of the original carbon catalyst and carbon samples produced during hydrocarbon (methane, propane and ethylene) decomposition. Carbon black BP-2000 with the surface area of 1500 m^2/g was used in these studies. Figure 11 depicts XRD spectra of the original carbon black (BP2000) sample and two different samples of carbon black (fine and coarse carbon particles) after exposure of CB to propane at 850°C.

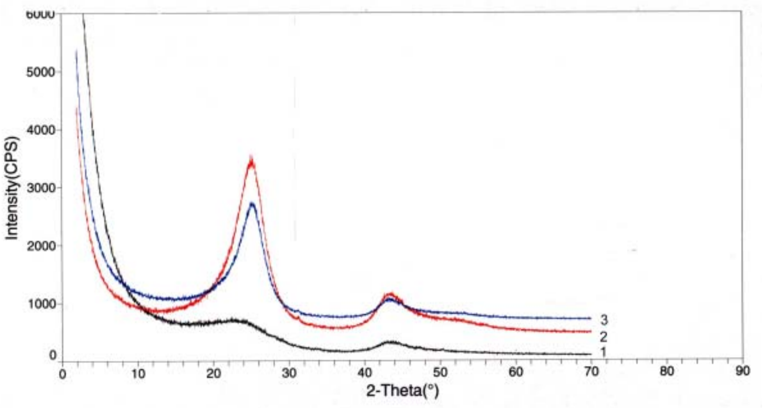

Figure 11. XRD Spectra of Carbon Samples. 1- original CB (BP2000), 2 and 3- samples of CB after exposure to C_3H_8 at 850°C (fine and coarse carbon particles, respectively)

In agreement with our earlier findings, the original carbon sample had one- or two-dimensional ordering, whereas, samples produced from hydrocarbon decomposition exhibited an order in the stacking (003) direction. The d-spacing (lattice spacing) is practically uniform, so that the

(003) columnar reflection is clearly present. The value of spacing between plates (d=3.49Å) is consistent with an ordered graphite-like or a turbostratic structure.

X-Ray Photoelectron Spectroscopic Studies of Carbon Samples

The results of X-Ray Photoelectron Spectroscopic (XPS) studies of different carbon samples are shown in Figures 12-14.

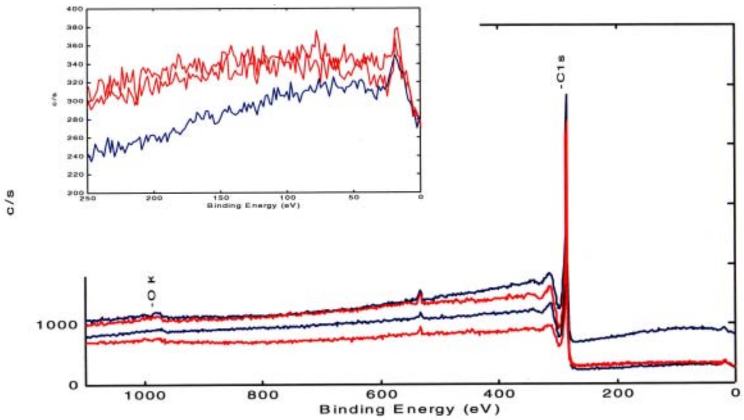

Figure 12. XPS Spectra of CB (BP2000) Samples Exposed to Propane at 850°C

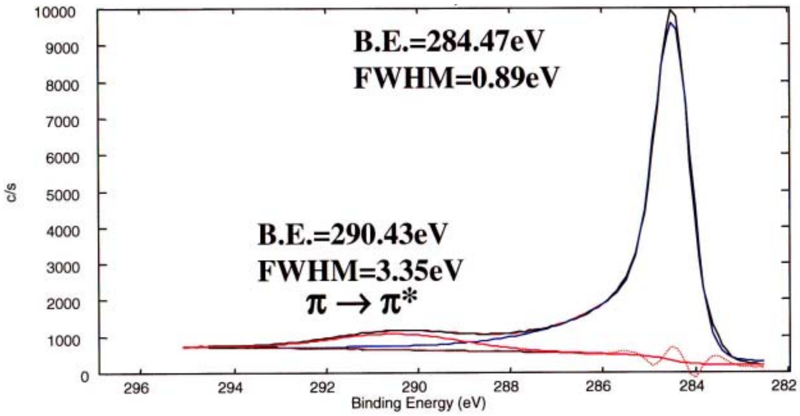

Figure 13. XPS Spectra of Carbon Samples. Peak Fitting of C1s Region for Original CB (BP2000)

The original carbon black (BP2000) showed trace amounts of silicone, sulfur and oxygen on its surface. Surface atomic concentrations are as follows (%): carbon- 98.6, oxygen- 1.0, sulfur- 0.2 and silicon- 0.1. Sulfur could result from the sulfur-containing aromatized petroleum fractions used in production of carbon black by the Furnace Black process. It can be seen from

Figure 12 that only trace amounts of oxygen are present on the surface of carbon particles produced by decomposition of propane over CB catalyst at 850°C

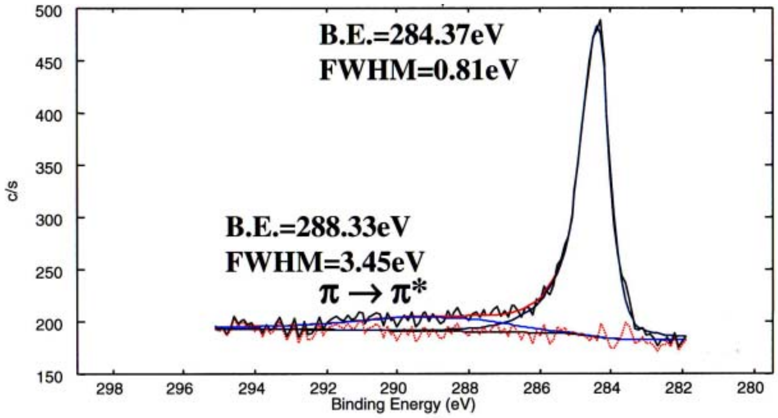

Figure 14. XPS Spectra of Carbon Samples. Peak Fitting of C1s Region for CB (BP2000) Samples Exposed to Propane at 850°C

It is clear from XPS spectra (see Figures 13,14) that there does not appear any distinction by XPS on the nature of original carbon and fine or coarse carbon particles produced by propane decomposition over CB (BP2000) catalyst. The carbon peak can be fit assuming the presence of graphitic-type carbon. It should be noted, however, that XPS is not very sensitive to the degree of the aromaticity of carbon (e.g., it can not differentiate between sp^3, sp^2 and sp carbon). The carbon in all the samples can be fit well assuming only one type of carbon.

Scanning Electron Microscopic Studies of Carbon Samples

Figure 15 depicts the SEM images of the original carbon black (BP2000) sample and the surface of a carbon particle produced by propane decomposition at 850°C. The SEM micrograph of the original CB sample clearly shows a fine structure of carbon black consisting of the agglomerates of small carbon particles (approx. 20 nm) (see Fig. 15 A). In contrast, the bulk of the surface of carbon particles produced by hydrocarbon decomposition consists of clusters and nodules 1-10 microns in diameter (Fig. 15 B). Prolonged (3-4 hours) exposure of carbon catalyst (CB BP2000) to a hydrocarbon stream at elevated temperatures (800-900°C) resulted in formation of spherical carbon particles with the dimensions in the range of 0.5-1.5 mm (Fig. 16 A).

It can be seen from the Figure 16 (A) that a crashed spherical particle (at the bottom) has a distinct layered structure. XRD analysis of the spherical carbon particles revealed that they exhibited an ordered graphite-like (turbostratic) structure similar to that of the above-described micron-size carbon particles.

It was found that the clusters of relatively thick carbon filaments are present on the surface of some spherical particles (not all of them). The carbon filaments have the diameter of approximately 1 micron, and are of the "octopus" type, with branches spreading out occasionally from the "main" filament (Figure 16 B). The common size of carbon nodules and filaments suggests that the nodules could be precursors to the filaments. It is apparent that carbon filaments arise when the available surface area is small, and the filaments growth is the only way to maintain a higher carbon deposition rate.

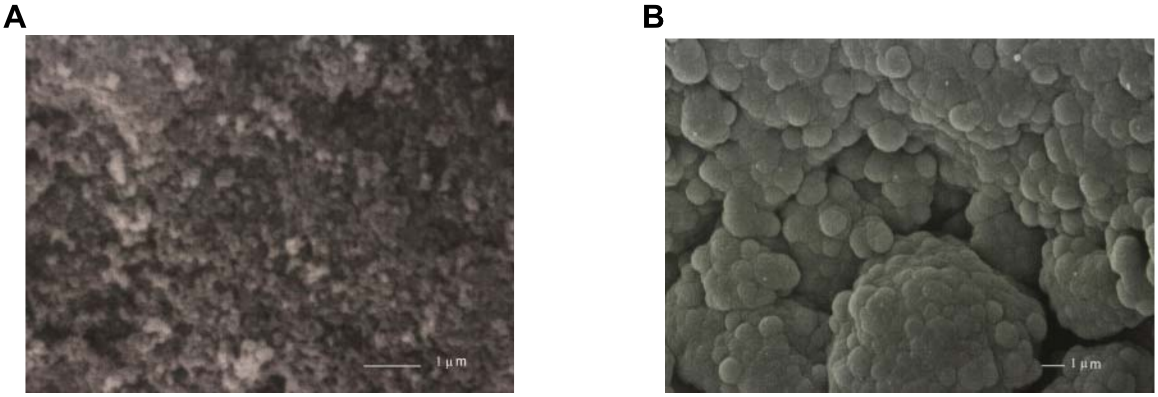

Figure 15. SEM Micrographs of Original CB BP2000 (A) and Carbon Sample Produced by Decomposition of Propane over CB BP2000 at 850°C (B).

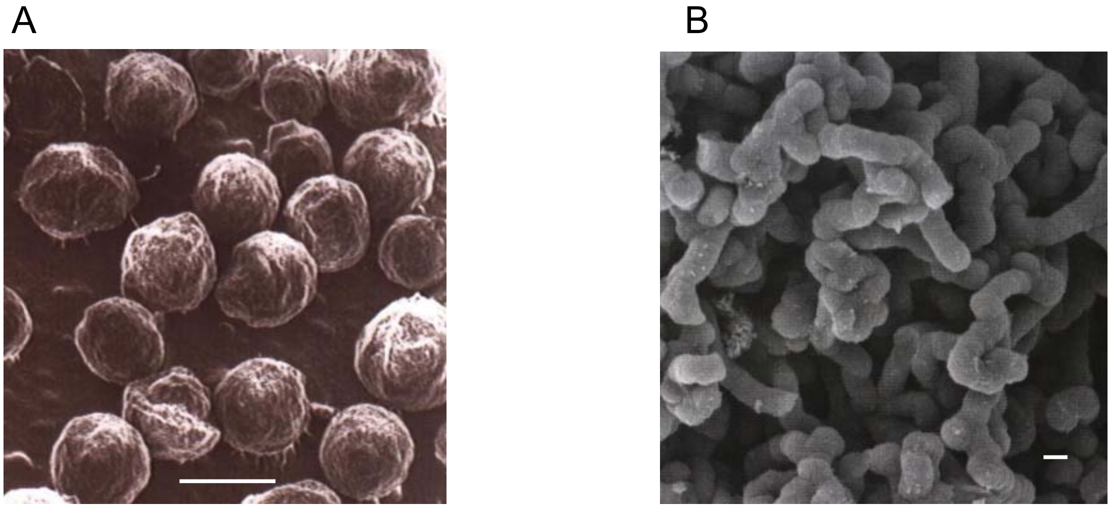

Figure 16. SEM Micrographs of Spherical Carbon Particles Produced by Decomposition of Propane over CB BP2000 at 850°C. A- View of Spherical Carbon Particles (scale bar- 1 mm), B- SEM of the Surface of Spherical Particles (scale bar- 1 µm)

Techno-economic Evaluation of Hydrogen Production by Thermocatalytic Decomposition of Natural Gas

Techno-economic analysis of hydrogen production by thermocatalytic decomposition of natural gas was conducted in cooperation with NREL. The two alternative technological approaches were analyzed: with the external and internal heat supply into the reactor. According to the first approach the technological scheme consisted of a fluidized bed catalytic reactor and a fluidized bed heater with carbon particles circulating between these two apparatuses (similar to the process of catalytic cracking or fluid coking). Process heat is provided by combusting a fraction of NG feed. Pressure swing adsorption (PSA) unit was assumed for the production of high purity hydrogen (>99 v.%). The hydrogen plants of different capacities were analyzed: small- 6, medium- 20 and large- 60 MMscfd.

The sensitivity analysis on the effect of carbon selling price on the hydrogen selling price was conducted. Figure 17 shows the hydrogen selling price as a function of carbon selling price for a small, a medium and a large hydrogen plants at NG selling price of $3.72 per GJ (internal rate of return, IRR, 15%).

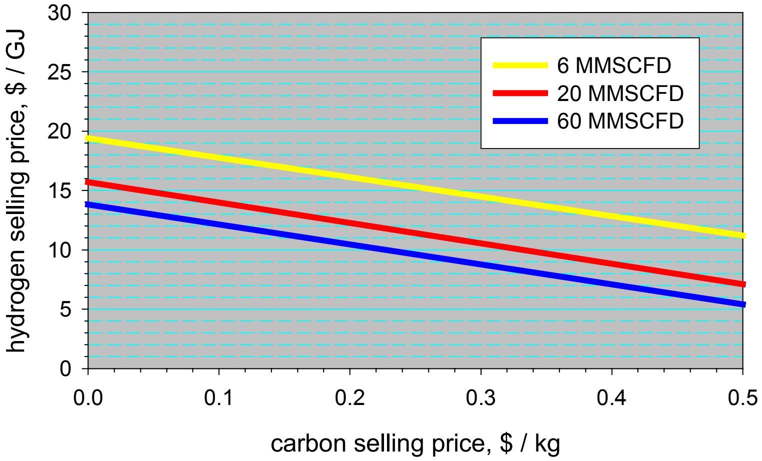

Figure 17. Hydrogen Selling Price vs Carbon Selling Price for Hydrogen Plants of Different Capacities (NREL) NG - $3.72 /GJ, IRR- 15%

It is evident that carbon credit could significantly reduce the cost of hydrogen production. Therefore, a great deal of consideration was given to the characterization of carbon-products of the process and evaluation of their market value. Based on the results of carbon products analysis it was concluded that one application area of our carbon product could be in metallurgical industry, e.g., the carbon electrodes for aluminum and ferro-alloys manufacturing. Currently, aluminum industry annually produces close to 4 mln ton of aluminum, with carbon (coke) consumption rate of 0.4-0.5 kg of carbon per kg of aluminum [10]. Thus, aluminum industry could be an important market for the ash-, sulfur- and metal-free carbon produced in TCD process with the selling prices of $0.30 per kg and higher. It can be derived from the Figure 17 that at carbon price of $0.30/kg hydrogen could be produced at the selling price of approx. $8/GJ which is comparable with the current selling prices for hydrogen produced by steam reforming of natural gas. It should be noted that hydrogen selling prices would be further reduced if a carbon credit for avoided CO_2 emissions were applied.

Although metallurgical and tire industries provide very important markets for the carbon products, it is realized that much larger markets should eventually be developed in order to economically justify the large scale production of hydrogen via methane decomposition. Therefore we place a strong emphasis on the development of new application areas for the carbon products. Our experimental results indicated that depending on the operational parameters of hydrocarbon decomposition process several valuable forms of carbon could be obtained, e.g., pyrolytic graphite, spherical carbon particles, carbon filaments and others. The selling prices for these modifications of carbon are well above $1/kg. The studies on the market value and new application areas for carbon products produced by catalytic methane decomposition are in progress.

Acknowledgements

This work was supported by the U.S. Department of Energy Hydrogen Program under the contract No. DE-FC36-99GO10456. The author also acknowledges the contribution of the Universal Oil Products, National Renewable Energy Laboratory, CREOL and Materials Characterization Facility of the University of Central Florida, Florida Institute of Technology, and AMIA Laboratories (Rigaku).

References

1. M. Steinberg. Fossil Fuel Decarbonization Technology for Mitigating Global Warming. *International Journal of Hydrogen Energy*, v. 24, p. 771, 1999.

2. M. Calahan. Catalytic Pyrolysis of Methane and Other Hydrocarbons. *Proceedings of Conference on Power Sources.* v. 26, 181, 1974.

3. F. Solymosi, A. Erdohelyi, A. Csereyi, A. Felvegi. Decomposition of CH_4 over supported Pd catalysts *J. Catalysis,* 147: 272 (1994)

4. M. Pourier, C. Sapundzhiev. Catalytic decomposition of natural gas to hydrogen for fuel cell applications, *Int. J. Hydrogen Energy, 22:429* (1997)

5. M. Callahan. Hydrocarbon fuel conditioner for a 1.5 kW fuel cell power plant. *Proceedings of 26th Power Sources Symposium,* Red Bank, N.J, 181 (1974)

6. N. Muradov. CO_2-free Production of Hydrogen by Catalytic Pyrolysis of Hydrocarbon Fuels. *Energy & Fuels*, v.12, p.41, 1998

7. N. Muradov. Catalysis of Methane Decomposition over Elemental Carbon. *Catalysis Communications,* No.2, 89, 2001

8. N. Muradov. Hydrogen via Methane Decomposition: an Application for Decarbonization of Fossil Fuels. *International Journal of Hydrogen Energy*, v.26, 1165, 2001

9. P. Tesner. Kinetics of Pyrolytic Carbon Formation. *Kinetics and Catalysis Series.* VINITI. Moscow, 1987.

10. Kirk-Othmer. *Encyclopedia of Chemical Technology*. J.Wiley & Sons, 1992